Comparison of CPTEC GCM and Eta Model Results with Observational Data from the Rondonia LBA Reference Site, Brazil

Sin Chan CHOU, José A. MARENGO

Center for Weather Prediction and Climate Studies—CPTEC, National Institute for Space Research—INPE, Cachoeira Paulista, SP, 12630-000, Brazil

Claudine P. DERECZYNSKI, Patricia V. WALDHEIM

Federal University of Rio de Janeiro (UFRJ), Rio de Janeiro, Brazil

and

Antonio O. MANZI

National Institute of Amazonian Research (INPA), Manaus, Brazil

(Manuscript received 7 February 2006, in final form 6 November 2006)

Abstract

We compared forecasts of the Center for Weather Prediction and Climate Studies (Centro de Previsão de Tempo e Estudos Climáticos—CPTEC) General Circulation Model (GCM) and the mesoscale Eta Model with observations undertaken at the Rondonia Coordinated Enhanced Observing Period (CEOP) reference site, Brazil, for the dry period between 1 July and 1 September 2001. The Rondonia site is located in the Jaru Biological Reserve Area in the state of Rondonia within the Amazon region. The site is forested and is one of the Reference Sites of the Large-Scale Biosphere–Atmosphere Experiment in the Amazon Basin (LBA) Continental-Scale Experiment (CSE). Time series and mean diurnal cycles of precipitation, near-surface temperature, latent and sensible heat fluxes, surface incoming shortwave and net radiation fluxes are shown for 24-h and 48-h forecasts. In the global model, the predicted incoming shortwave radiation and net radiation are similar to observed values; however, this is accompanied by large overestimate of deep clouds and precipitation. Partition of the available energy results in an overestimate of the sensible heat fluxes and an underestimate of the latent heat fluxes. The latent heat fluxes are large shortly after rain, but decay quickly. No clear improvement is noted in the 48-h forecasts compared with the 24-h forecasts.

The Eta Model is a grid-point limited-area model. Its precipitation forecasts are similar to observations; however, the model overestimates the incoming shortwave radiation, resulting in excessive net radiation. The Eta sensible and latent heat fluxes are both overestimated, and 48-h forecasts produce small improvements over the 24-h forecasts. Near-surface temperatures are overestimated by both models. The global model requires a reduction in precipitation production, and both models require a reduction in incoming short-wave radiation at the surface.

Corresponding Author: Sin Chan Chou, Center for Weather Prediction and Climate Studies—CPTEC, National Institute for Space Research—INPE, Cachoeira Paulista, SP, 12630-000, Brazil.

1. Introduction

The measurement of energy, momentum, and moisture fluxes at the earth's surface is important in gaining an understanding of the energy and water cycle in the climate system. Numerical models are generally used to simulate the transfer of energy and water between the land and atmosphere; however, models contain biases related to numerical limitations in terms of resolution and the physics and dynamic schemes employed in the model. A description of model errors can help to identify sources of error and potential improvements to the model schemes, thereby producing more realistic model simulations. The reliability of results obtained using model output depends on the magnitude of the model error and the character of the error pattern.

The objective of the present work is to compare forecasts of the CPTEC GCM and Eta Model with surface observations collected at the Rondonia Site for the period between 1 July and 1 September 2001. This is a forested site located at 10°04′42″S, 61°56′2″W in the Jaru Biological Reserve Area in the Rondonia State, Brazil. Hourly measurements of air temperature, precipitation, latent and sensible heat fluxes, incoming shortwave and longwave radiation, and outgoing shortwave and longwave radiation were obtained at the site. The verifying models are used operationally at CPTEC and represent a contribution by CPTEC to CEOP (Coordinated Enhanced Observing Period; Bosilovich and Lawford 2002).

Global models generally use a coarse spatial resolution within which sub-grid-scale phenomena are represented by parameterization schemes. Mesoscale models are applied to add detail in describing surface characteristics such as topography, vegetation, and soil conditions, and to improve representations; however, such models have their limitations, as they require parameterization of physical processes and must take into account errors associated with the lateral boundary conditions. The evaluation of such models is important because they are increasingly used as research tools for understanding past and future climate conditions.

Intercomparison projects such as the Atmospheric Model Intercomparison Project (AMIP) (Gates et al. 1998) and the Project to Intercompare Regional Climate Simulations (PIRCS) (Takle et al. 1999) were designed to establish standardized frameworks for numerical experiments involving general circulation models and regional climate models, respectively. A comparison of model results can identify the deficiencies of the employed models. For example, the ensemble mean precipitation produced from the 25 AMIP models shows large inter-model differences at low latitudes, although the simulation results are similar to observations. These models are also deficient in terms of simulating total cloudiness.

In Brazil, several observation sites are available for verification against model outputs as part of the Large-Scale Biosphere–Atmosphere Experiment in the Amazon Basin (LBA) Continental-Scale Experiment (CSE) reference site network. A forest site in Rondonia State, Brazil (Jaru Biological Reserve), measures both the major variables such as the 2-m temperature and 10-m wind and surface fluxes. Flux verifications are important because they reveal the model's partitioning of energy.

The partitioning of energy between latent and sensible heat is one of the major sources of error in weather and climate simulations (Betts et al. 1996). Land-surface schemes driven by observed conditions can produce realistic simulations, such as the results obtained using the Simplified Simple Biosphere Model (SSiB) over the Amazon Basin (Xue et al. 1991; Xue et al. 1996); however, model errors can arise when the land-surface schemes are coupled to atmospheric models, as the interaction with other schemes within the model can lead to greater errors. In the validation of the Eta/SSiB Model over South America, Chou et al. (2002) found that an overestimate of the surface latent and sensible heat fluxes could result from excessive incoming shortwave radiation reaching the surface. This excessive shortwave radiation was also found in short-range forecasts over North America (Betts et al.1997). This error might reflect cloud treatment or deficient extinction by water vapor or aerosols in the model, as suggested in an evaluation of the National Centers for Environmental Prediction (NCEP) Eta Model using Atmospheric Radiation Measurement (ARM) data (Hinkelman et al. 1999).

The evaluation of Eta Model precipitation forecasts over South America carried out by Bustamante et al. (1999) showed that the 24-h precipitation forecasts are less accurate than the 36-h or 48-h forecasts. Their evaluation was based on a rainy month for the Amazon region. The improvement of the forecast within this short range indicates the poor quality of the initial conditions: the dependence of the quality of the forecasts on the initial conditions is stronger in short-range forecasts. A comparison of the errors at 24 h and 48 h can help to indicate the rate at which the errors propagate in the model.

Although in the present study verification is carried out against a point measurement, the site is located within a homogeneous forest area; therefore, the measurement values can be regarded as being approximately representative of the wider area.

The remainder of the present paper is organized in the following sections. The analyzed models are described in Section 2 and site characteristics are outlined in Section 3. Model verifications are presented in Section 4, and the main conclusions of the study are drawn in Section 5.

2. Models

2.1 CPTEC GCM

The version of the CPTEC GCM used in this work is a spectral model with triangular truncation T126 and 28 layers in the vertical (Bonatti 1996). This horizontal resolution is approximately equivalent to a 100 $\times$ 100 km grid. The first layer is approximately 60 m thick, and the model uses a sigma vertical coordinate. Convective precipitation is produced by the Kuo scheme as modified by Anthes and Keyser (1979). Land-surface energy transfers are resolved using SSiB (Xue et al. 1991), which maps 12 types of vegetation cover. Calculations of shortwave radiation are performed every 2 h based on the scheme developed by Lacis and Hansen (1974). The longwave radiation fluxes are calculated every 3 h and are based on the scheme of Harshvardhan et al. (1987). The model-verification grid box at the Jaru Biological Reserve has an evergreen forest type of vegetation. Albedo was obtained from seasonal climatology, and sea-surface temperatures were taken from weekly mean values updated daily on a $1^\circ \times 1^\circ$ grid. Monthly climatology provided the initial conditions for soil moisture, and the initial atmospheric conditions are taken from NCEP analyses at T126L28. Additional details on the CPTEC GCM and its validation can be found in Cavalcanti et al. (2002) and Marengo et al. (2003).

2.2 Eta Model

The Eta Model (Mesinger et al. 1988) is the limited-area model used operationally at CPTEC. The model uses the Eta vertical coordinate (Mesinger 1984), and prognostic variables are temperature, horizontal winds, specific humidity, surface pressure, turbulent kinetic energy, and cloud hydrometeors. Convective precipitation is produced using the Betts–Miller–Janjic scheme (Betts and Miller 1986; Janjic 1994), and land-surface processes are treated using the Noah Land Surface Model (Chen et al. 1997). The verification grid-box for the Eta Model in the Jaru Biological Reserve Area also has an evergreen forest vegetation-type and an elevation of 63 m. The radiation package was developed by the Geophysical Fluid Dynamics Laboratory in Princeton, the United States. Model shortwave radiation is treated using the Lacis and Hansen (1974) scheme, whereas longwave radiation is treated using the Fels and Schwarzkopf (1975) scheme. The longwave and shortwave fluxes are calculated every model hour. The initial atmospheric conditions are taken from NCEP analyses at T126L28, which are the same as those used by the CPTEC GCM, and the lateral boundaries are updated every 6 h from CPTEC GCM forecasts. The Eta Model used a seasonal climatological albedo and daily updated sea-surface temperature, as used by the global model. The initial soil moisture was taken from the 12-h forecast of the global model, and the model was configured with 20-km resolution and 38 layers. At this resolution and with the use of an updated vegetation map (Sestini et al. 2002), the model is able to identify the notorious arc of deforestation at the southern boundary of the Amazon region, which extends close to the surrounding area of the Jaru Biological Reserve Area.

3. Site characteristics

The CEOP initiative is currently in the process of firming up the contributions of the atmospheric modeling centers to the CEOP archive center for model data. The LBA project is part of the Global Energy and Water Cycle Experiment (GEWEX) CSEs around the world, and

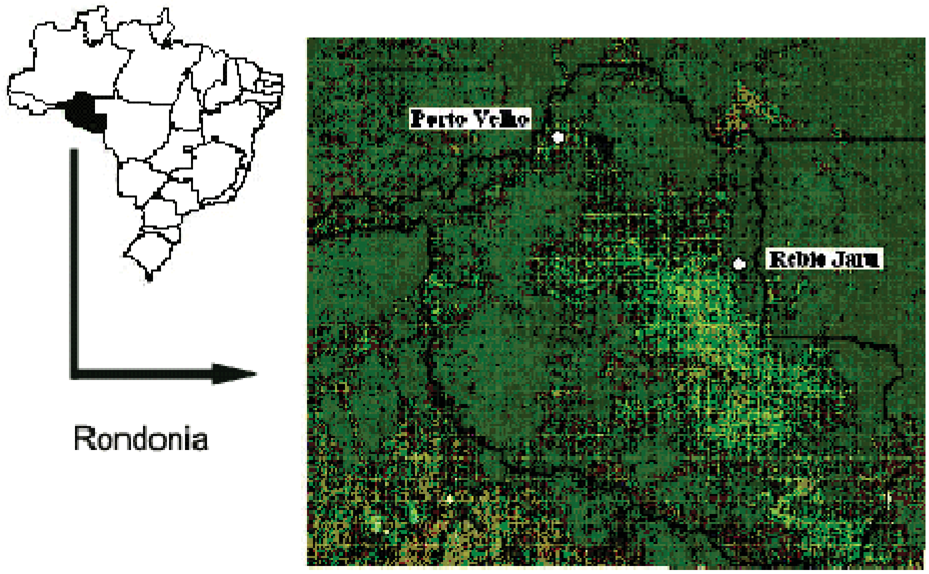

Fig. 1. Location of the Jaru Biological Reserve in Rondonia State, North Brazil.

CPTEC is the main operational center where LBA modeling activities are developed. As part of the CEOP program, each CSE maintains a number of reference sites that consist of experimental sites with flux towers that undertake observations at high temporal resolutions. Among the reference sites available in the LBA region (Marengo and Horta 2003), the chosen station possesses the most complete dataset.

The observations are taken from the tower located in the Rondonia site where the vegetation cover is mainly evergreen tropical forest. The Ji-Paraná River flows next to the reserve and the topography in the area varies in elevation from 0 to 800 m. Figure 1 shows the location of the reference site.

The Rondonia site has not been in operation long enough to produce a reliable climatology; thus, the climatology was estimated from the nearest conventional surface station located at Porto Velho (8°27′36″S, 63°03′00″W and 95 m a.s.l.), which is approximately 250 km from the Rondonia site. The mean temperature in Porto Velho during July and August is 24–25°C. These two months are the coldest of the year, with average minimum temperatures of approximately 18 and 19°C, respectively, which result from cold fronts that occasionally reach this far north. The largest diurnal temperature range of the year occurs during these two months, as the average maximum temperatures reach 31°C in July and 33°C in August. During 2001, the temperatures were slightly higher than the normal mean. The Rondonia climatological total precipitation in July is about 23 mm, which on average falls on only 2 rainy days (Rebello et al. 1996); this is the driest period of the year in this region. In 2001, 34.5 mm of precipitation was observed at the Rondonia site in July and 0 mm in August. During the study period, there were only 3 days on which rain was recorded at the reference site. Table 1 shows the monthly observed precipitation for the period; most of the precipitation occurred in one event on 25 July 2001.

Table 1. Monthly total precipitation [mm] derived from observations, CPTEC GCM 24-h and 48-h forecasts, and Eta Model 24-h and 48-h forecasts.

Month	Observation	CPTEC GCM		Eta Model	
		24-h	48-h	24-h	48-h
July	34.6	121.5	154.9	2.1	0.2
August	0.0	27.3	140.8	0.0	1.5

4. Verification

The Rondonia reference site provided observations of precipitation, 2-m air temperature, surface winds, latent and sensible heat fluxes, downward and upward shortwave and longwave radiation and net radiation. Here, we verify the variables related to the surface heat balance. Because the global model operationally writes output every 6 h, the predicted precipitation was accumulated every 6 h, whereas the energy fluxes were averaged over each 6-h period. The forecasts of the Eta Model were output every hour.

While the comparison between the grid-box value of the model and the value at the observation point may not be completely fair, it is still expected that the spatial homogeneity of the forest site may enable it to approximate an area-mean value and thereby be comparable to the coarse-scale model grid values. It is expected that systematic errors may provide some indication of the model processes that generate the errors. We compared the forecasts of the CPTEC T126L28 GCM and the Eta Model at 20-km resolution. This latter model is driven via the lateral boundaries by the global model conditions.

Time series of the variables measured at the site for 24-h and 48-h model forecasts may reveal some dependence of forecast quality on the initial conditions and model errors. Both models take initial conditions from the NCEP analyses at T126 truncation and 28 sigma levels. The spectral truncation of the global model results in the Gibbs effect in grid space due to the proximity of Rondonia State to the Andes Mountains; this effect is evident in the verifications. The global model elevation of the grid box that contains the reference site is 280 m. The formulations of the dynamics and physics in the two operational models are distinct; thus, different errors can be expected from the models even though both start from the same initial conditions and one of the models is driven by the other via the lateral boundaries.

Forecast error statistics were calculated based on bias, root mean square error (*RMSE*), and correlations between forecast and observed time series. The standard deviation of the series was also calculated to provide a measure of the variability of the evaluated variables. The bias, or the part of the mean error that remains after the cancellation of compensating errors, indicates the offset of the forecasts compared to observations. The rmse penalizes the large errors and is generally larger in higher-resolution models due to their inherently larger internal variability. It is expected that rmse will show a small growth rate in the forecasts from 24 h to 48 h. The linear correlation indicates the degree to which the forecast series are in phase with observations. These statistics were chosen for their simplicity in terms of revealing the magnitude of error features.

4.1 Precipitation

Precipitation was observed at the Rondonia site on 3 days, which is close to the climatological number of rainy days recorded in nearby Porto Velho. These rain events were caused by isolated convection on 25 July 2001 and the passage of a frontal system over the southeastern part of the continent on 27–28 July 2001. The accumulated precipitation was 28.6 mm on 25 July, 4.2 mm on 27 July, and 3.8 mm on 28 July. The frontal cloud band extended toward Rondonia, causing precipitation and a sharp decrease in temperature on those days; no rain was observed during August 2001.

Figure 2 shows the brightness temperature estimated from infrared satellite channels. According to Machado et al. (1998), a deep convective cloud system can be identified from infrared brightness temperatures below $-28°$C, and at some time this may contain embedded convective clusters that are defined by values below $-55°$C. The event caused by deep convection was that of 00Z 25 July, when brightness temperatures reached values below $-30°$C. On 27 and 28 July, the total precipitation amounts were smaller and the cloud tops remained below the $-30°$C isotherm; cloud-free periods were common.

The forecasts of the global model clearly overestimated the number of precipitation events, as forecasts produced rain in most of the days in July and toward the end of August (Fig. 3). Precipitation amount tended to increase with time during the forecasts in August, as shown by the 48-h forecasts (Fig. 3). The large-scale organization induced by the frontal passage triggered isolated convective showers in Rondonia. The overestimate of pre-

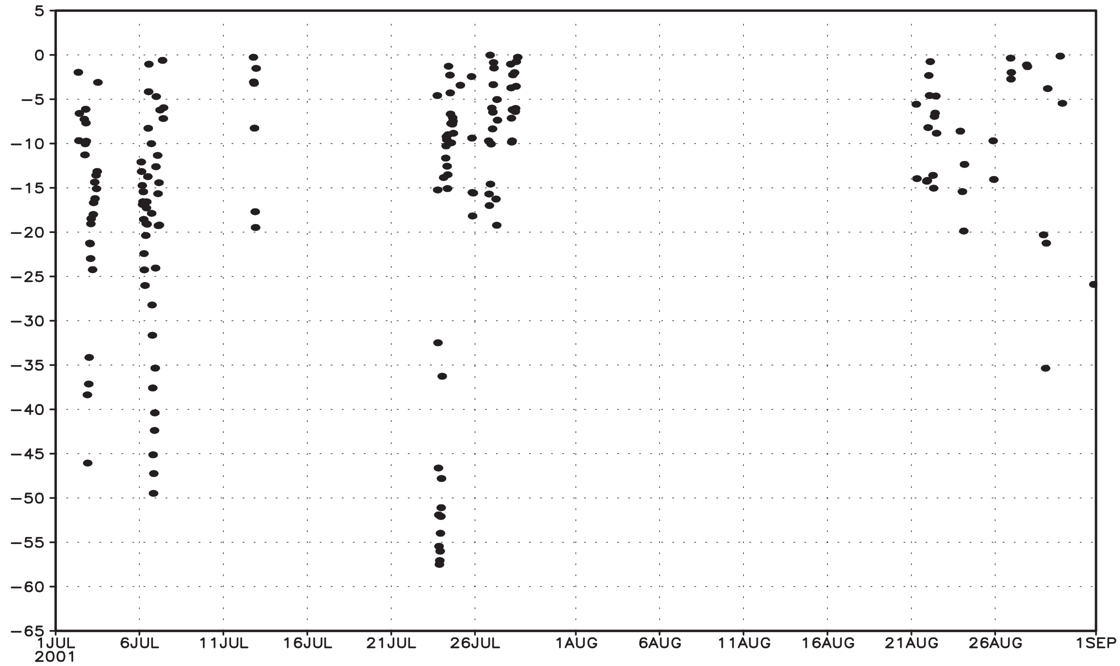

Fig. 2. Brightness temperature below 0°C taken around the Rondonia reference site. Values below −30°C are considered to be high-top clouds.

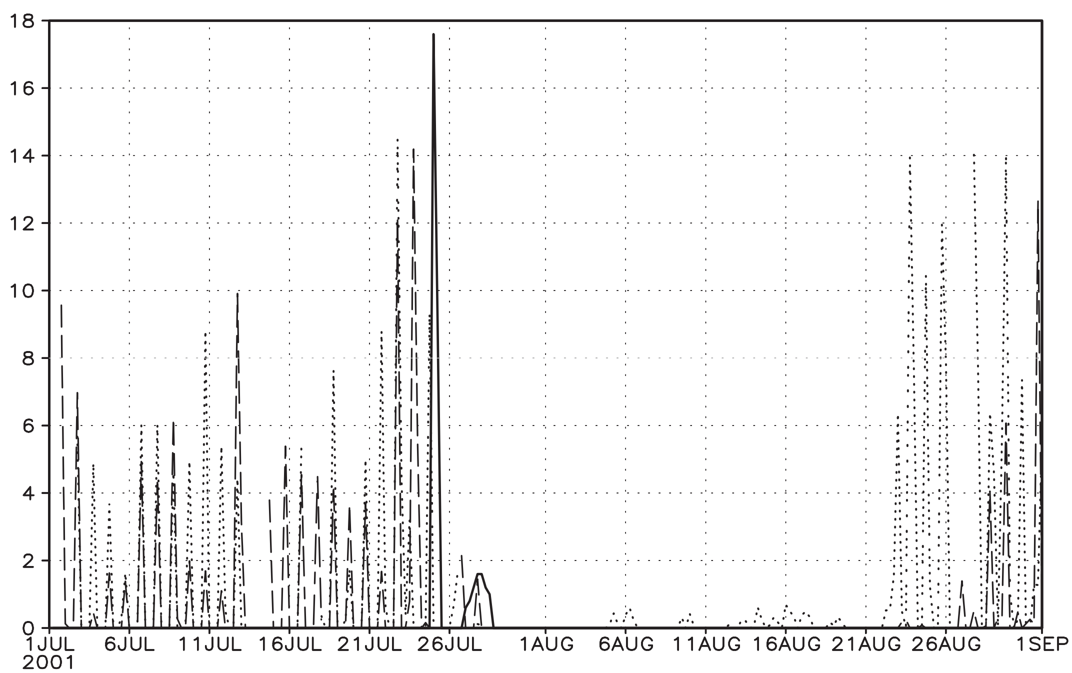

Fig. 3. Six-hourly accumulated precipitation [mm] derived from observations (thick line) and Global Model 24-h (dashed line) and 48-h (dotted line) forecasts.

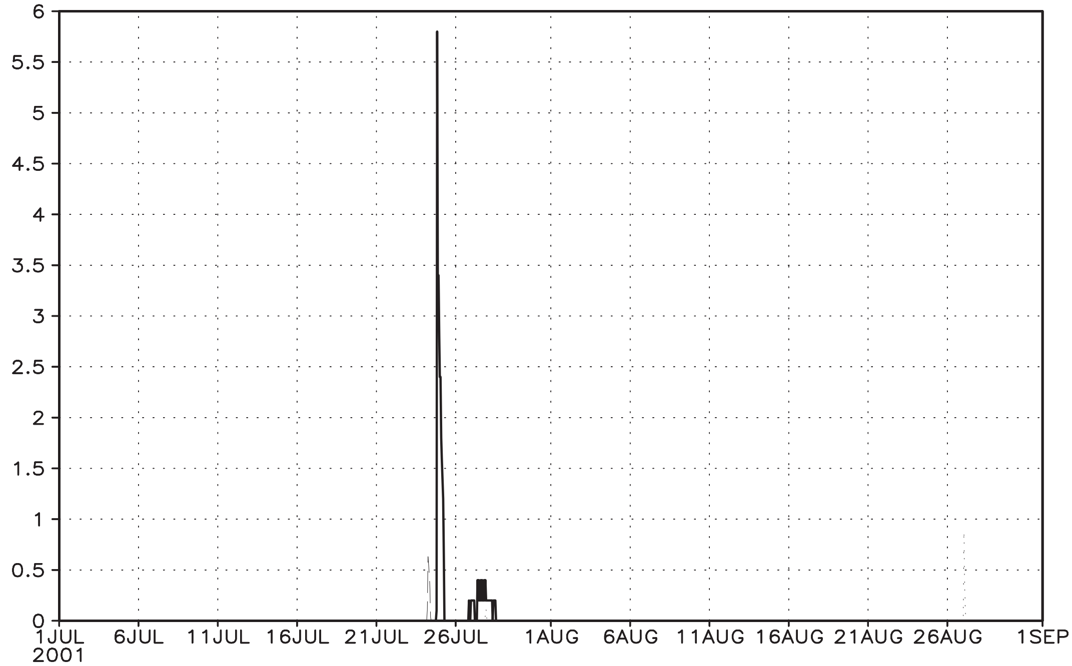

Fig. 4. Hourly accumulated precipitation [mm] derived from observations (thick line) and Eta Model 24-h (dashed line) and 48-h (dotted line) forecasts.

cipitation events in the global model may reflect its coarse horizontal resolution (grid size of approximately 100 km × 100 km). The model may also have attempted to include precipitation at neighboring sites; nonetheless, the total accumulated monthly precipitation predicted by the global model is much larger than observed values (Table 1). The accumulated precipitation of the global model in July was approximately 121 mm for the 24-h forecasts and 155 mm for the 48-h forecasts, whereas the observed accumulated precipitation was about 35 mm.

In contrast, the Eta Model produced just one rain event in the 24-h forecasts (Fig. 4) for the study period, which is more similar to the observed frequency in the region. However, the 48-h forecasts (Fig. 4) produced two precipitation events and smaller total amounts, which suggests that no increase in the precipitation amount with integration is recorded in the Eta Model.

The total monthly precipitation values of the Eta Model are more similar to observed values, but remain below observations for July and above observations for August (Table 1). The no-rain events were accurately forecast by the Eta Model, as the number of rain events was close to the observed number. The global model uses a different convection scheme to that used in the Eta Model, and this results in distinct precipitation patterns predicted by the two models. July and August are the driest months for this region. During this time, precipitation events result from showers related to frontal passages to the south, although these events were not well captured by the models. An evaluation of the precipitation forecasts of the Eta Model for the rainy month of April revealed that the model started with large precipitation-forecast errors for 24-h forecasts, but the error decreased with integration at 36 and 48 h (Bustamante et al. 1999).

4.2 Latent heat flux

The global model predicted a latent heat flux for July that was similar to observed values; however, these fluxes were largely underestimated in August (Fig. 5). The model produced frequent precipitation in July but rare precipitation in August. There appears to be an inverse relation between the error in the forecast

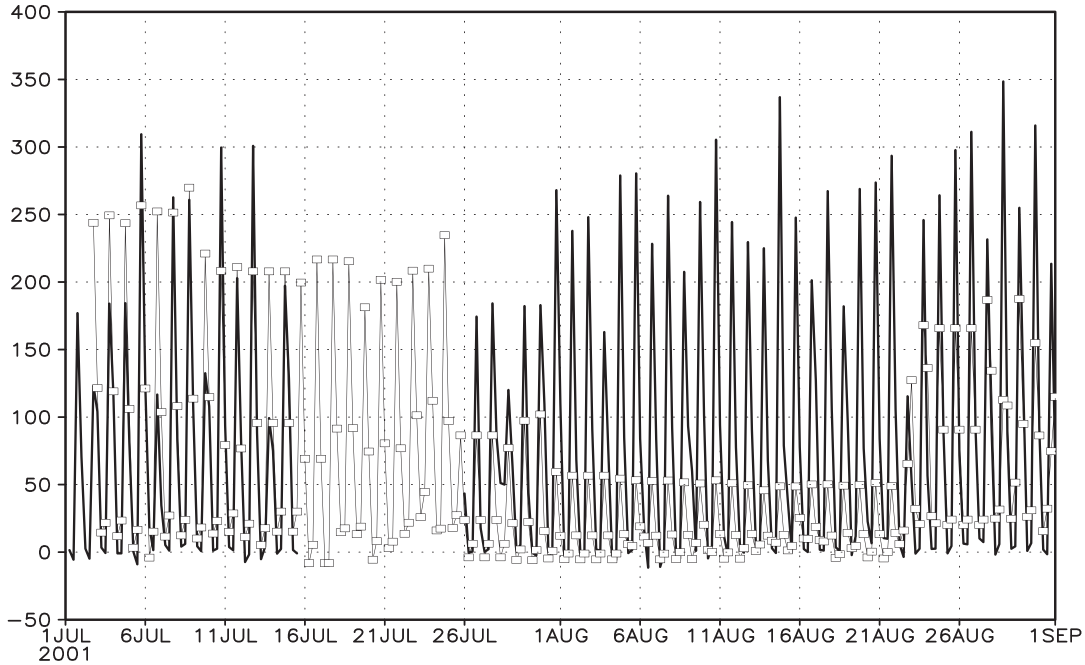

Fig. 5. Latent heat flux [W m^{-2}] derived from 6-h mean observations (thick line) and 48-h global model forecasts (squares). Observations were not collected during the period 16–26 July 2001.

latent heat flux and the amount of precipitation. Although the model contains a large bias in its July precipitation forecasts, the latent heat fluxes for July are closer to observed values. In late July, when observational data were missing, the model results were of approximately the same magnitude as those for the early part of the month; however, when the model ceased its precipitation production, these fluxes decreased sharply. This trend is clearer in the 48-h forecasts for August when the latent heat fluxes reached their minimum before increasing again after 24 August as the model rains resumed. During days without rain, no water was supplied to the surface from precipitation, leading to a reduction in the latent heat fluxes. This may indicate an inefficiency in the model land-surface scheme in terms of producing direct evaporation or in terms of producing evapotranspiration from the vegetation by extracting soil moisture from deeper layers at shorter time scales during dry days. In the global model, a sharp depletion in soil moisture occurred immediately after the rains ceased. Figure 6 shows the sharp depletion in surface soil wetness in the global model, which may indicate a rapid transfer of water or loss of water to the drainage zone.

In contrast to the global model, the latent heat fluxes predicted by the Eta Model exceeded the observed values at the Rondonia site. The model fluxes showed a smaller degree of temporal variability than the observations. This is shown in Table 2, where the standard deviation of the forecasts is smaller than that of the observations. The forecast fluxes slowly decreased toward the end of the dry season. The 24-h forecasts remained below values of approximately 400 W m^{-2}, whereas the hourly observations peaked at 600 W m^{-2} on several occasions. During late July, when observations were not recorded, the model results peaked at about 450 W m^{-2}; this is similar to values for the early part of the month. The errors in the Eta Model were different from those in the global model, as the magnitude of the Eta fluxes were maintained, regardless of the amount of precipitation. Figure 6 shows that soil wetness of the Eta Model remained at higher values than that of the global model during early August when both models produced no rain.

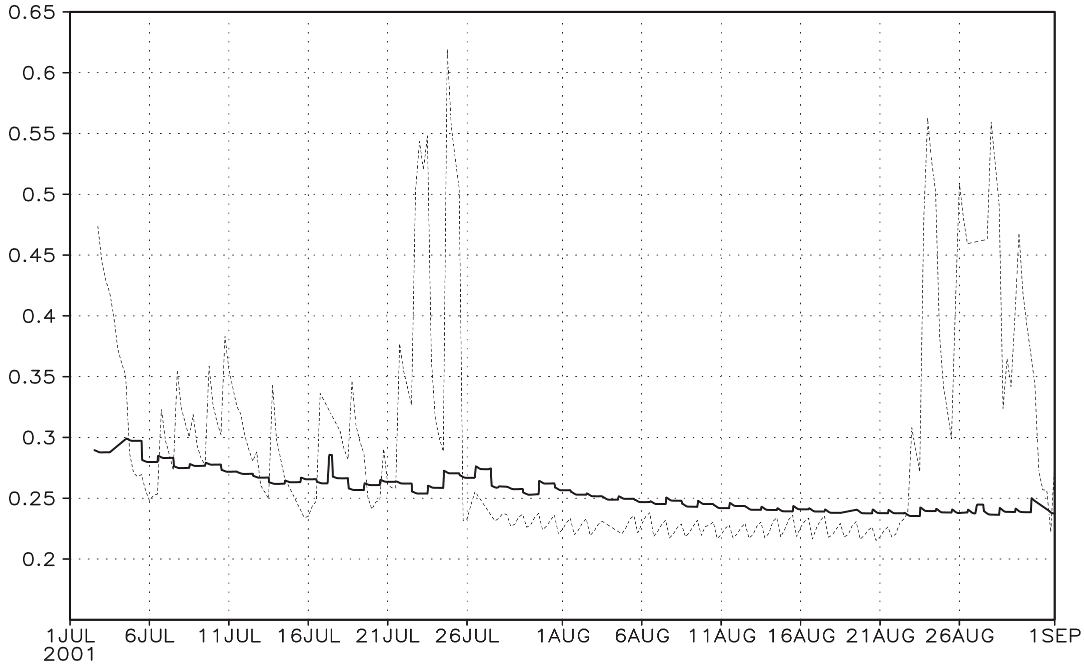

Fig. 6. 48-h Global (thin solid line) and Eta (thick solid line) forecasts of soil wetness (dimensionless) in the surface layer.

Table 2. Standard deviation, bias error, root mean square error and correlation between observations and CPTEC GCM and Eta Model forecast time series of latent heat flux [W m^{-2}].

Model	SD Obs	SD		BIAS		RMSE		CORR	
		24-h	48-h	24-h	48-h	24-h	48-h	24-h	48-h
CPTEC GCM	127.5	84.2	70.3	−19.6	−27.7	97.3	114.0	0.67	0.50
Eta Model	98.7	160.9	158.3	43.3	40.8	93.1	92.0	0.86	0.85

Figure 7 shows the mean diurnal cycle of the latent heat flux calculated for the 2-month study period. The observed values were averaged over 6-h intervals to enable comparison with the global model quantity. The observed 6-h mean value at 18Z of about 240 W m^{-2} was underestimated by the global model at 24 h; the error increased at 48 h. Figure 8 shows that the error was produced by the forecasts in the second half of the period (in August) when the global model produced reduced precipitation and latent heat fluxes. As the global model produced little rain in August, the soil surface had less moisture available for evaporation and latent heat fluxes were underestimated. In July, the mean error in the latent heat flux was positive.

The mean observed peak value of approximately 310 W m^{-2} at 17Z was largely overestimated by the Eta Model forecasts, which yielded an average of approximately 420 W m^{-2} (Fig. 7). Unlike the global model, the Eta Model generally overestimated these fluxes. Table 2 shows that while the global model has a negative bias, the Eta Model has a positive bias. The 48-h Eta forecasts showed a small improvement relative to the 24-h forecasts, along with the opposite error-growth behavior of that in the global model. The large transfer coefficient may have caused the excess in surface

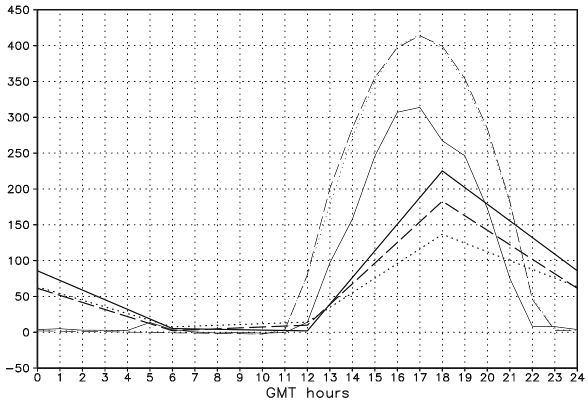

Fig. 7. Mean diurnal cycle of the latent heat flux [W m^{-2}] derived from 6-hourly mean observations (thick solid line), global model 24-h (thick dashed line) and 48-h (thick dotted line) forecasts, hourly observations (thin solid line), and Eta Model 24-h (thin dashed line) and 48-h (thin dotted line) forecasts.

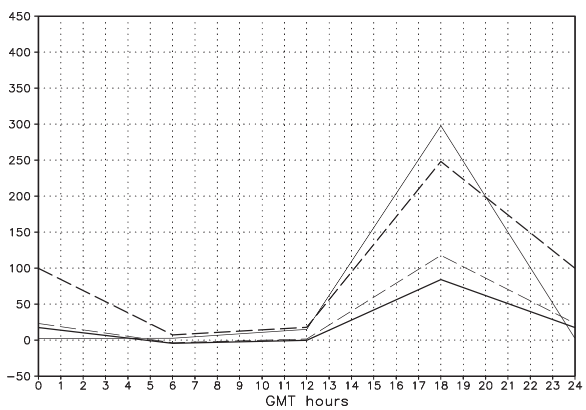

Fig. 8. Six-hourly mean diurnal cycle of latent heat flux [W m^{-2}] in July derived from observations (thick solid line) and 24-h global model forecasts (thick dashed line). Values are also shown for August derived from observations (thin solid line) and 24-h global model forecasts (thin dashed line).

heat fluxes; however, a reduction in the coefficient could aggravate the positive bias in the surface temperature.

Table 2 shows that the standard deviation of the observed 6-hourly mean latent heat flux is larger than the standard deviation of the global model forecasts for the July–August 2001 time series. This indicates that the model showed little temporal variability. The mean errors of the series were negative, and rmse increased from 24 h to 48 h in the forecasts. The correlations between global model forecasts and observed latent heat flux series were the smallest among the different fluxes. The standard deviation of the observed hourly mean latent heat fluxes was smaller than the standard deviation of the Eta Model forecasts. Unlike the global model, the mean error was positive, the *RMSE* showed little change at 48 h, and the correlation between observed and forecast series was approximately 0.85.

4.3 Sensible heat flux

Although observations were taken during dry periods, the sensible heat fluxes are smaller than the latent heat fluxes. While the mean hourly latent heat fluxes are approximately 300 W m^{-2}, the hourly sensible heat fluxes peak at about 120 W m^{-2}. The forest maintains evapotranspiration at a constant rate despite the lack of rain. This feature of the forest during dry days was also observed by Shuttleworth et al. (1984) in the first field measurements undertaken in Amazonia.

During the period in which precipitation was predicted by the global model, the sensible heat fluxes were comparable to observed values; however, in no-rain or reduced-rain periods, the global model largely overestimated these fluxes. This error may reflect the model deficient latent heat flux. The resulting increase in surface temperatures, due to reduced surface evaporation, led to an increase in surface sensible heat fluxes; this error is generated during dry days in the global model. As the integrations progressed to the 48-h forecasts, the global model showed a slight improvement in terms of these errors. The change in regime of the model fluxes occurred after 24 July, when the fluxes increased sharply as model rains ceased. In late July, when observations were missing, a gradual increase in the fluxes is apparent from the global model results.

The Eta Model forecasts of sensible heat fluxes also exceeded observed values. The model peak values of approximately 200 W m^{-2} generally exceeded the observed peak values. Model error in the sensible heat flux is consistent

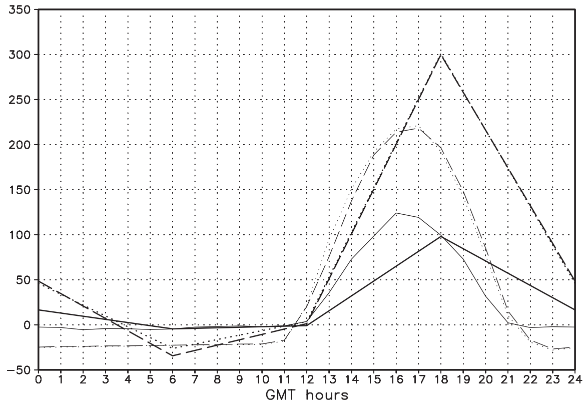

Fig. 9. Mean diurnal cycle of sensible heat flux [W m^{-2}] derived from 6-hourly mean observations (thick solid line), global model 24-h (thick dashed line) and 48-h (thick dotted line) forecasts, hourly observations (thin solid line), and Eta Model 24-h (thin dashed line) and 48-h (thin dotted line) forecasts.

with the large positive error in near-surface air temperature described below. The Eta Model showed a decrease in the daily maxima of sensible heat fluxes toward the month of August, which was the opposite trend to that for the latent heat flux; this trend is not clear in the observations.

The mean diurnal cycle of the sensible heat fluxes (Fig. 9) reveals that the global model overestimated these fluxes, mainly at 18Z. This error appears to arise progressively during the predicted no-rain periods in August when the fluxes were overestimated. At 18Z, the observed 6-hourly mean value was approximately 100 W m^{-2}, whereas the forecasts peaked at approximately 300 W m^{-2}. Both the 24-h and 48-h mean forecasts of the global model show similar values. The time of 18Z is equivalent to 1400 local time for Rondonia, which is the time that deep clouds are fully developed and most of the convective precipitation is observed (Negri et al. 2002). In August, the model produced larger sensible heat fluxes. The sensible heat fluxes of the global model are much larger than the latent heat fluxes; this is an undesired feature for this forest.

The mean diurnal cycle of the sensible heat flux of the Eta Model (Fig. 9) summarizes the overestimated fluxes for the study period. During the daytime, these predicted fluxes exceeded observed values, but the peaks were in phase. During the nighttime, the predicted fluxes generally became negative, indicating an excessive surface inversion at these times. Daily negative fluxes are recoded in the observed data, although these are cancelled out over the duration of the study period. As expected, the Eta sensible heat fluxes are smaller than the latent heat fluxes for the duration of the study period.

Table 3 shows that the sensible heat flux series of both the global model and the Eta Model record greater variability than observed data (as indicated by the standard deviations). The biases of these fluxes were positive for both models. The *RMSE* for the Eta forecasts were much smaller than those for the global model errors. For both models, there is little change from 24-h to 48-h forecasts.

4.4 Radiation

The observed 6-hourly mean incoming shortwave radiation showed values peaking at approximately 700 W m^{-2}. Smaller values were predicted in July, indicating cloudy conditions more often than those in August. The global model incoming shortwave radiation predicted at 24-h or 48-h lead times showed values comparable to observed data for July. These fluxes were overestimated in August, mainly during the period when the model did not produce

Table 3. Standard deviation, bias error, root mean square error and correlation between observations and CPTEC GCM and Eta Model forecast time series of sensible heat flux [W m^{-2}].

Model	SD Obs	SD		BIAS		RMSE		CORR	
		24-h	48-h	24-h	48-h	24-h	48-h	24-h	48-h
CPTEC GCM	51.9	152.2	150.5	66.5	64.7	142.6	138.1	0.77	0.79
Eta Model	41.7	92.5	92.7	14.9	17.0	58.8	61.3	0.83	0.83

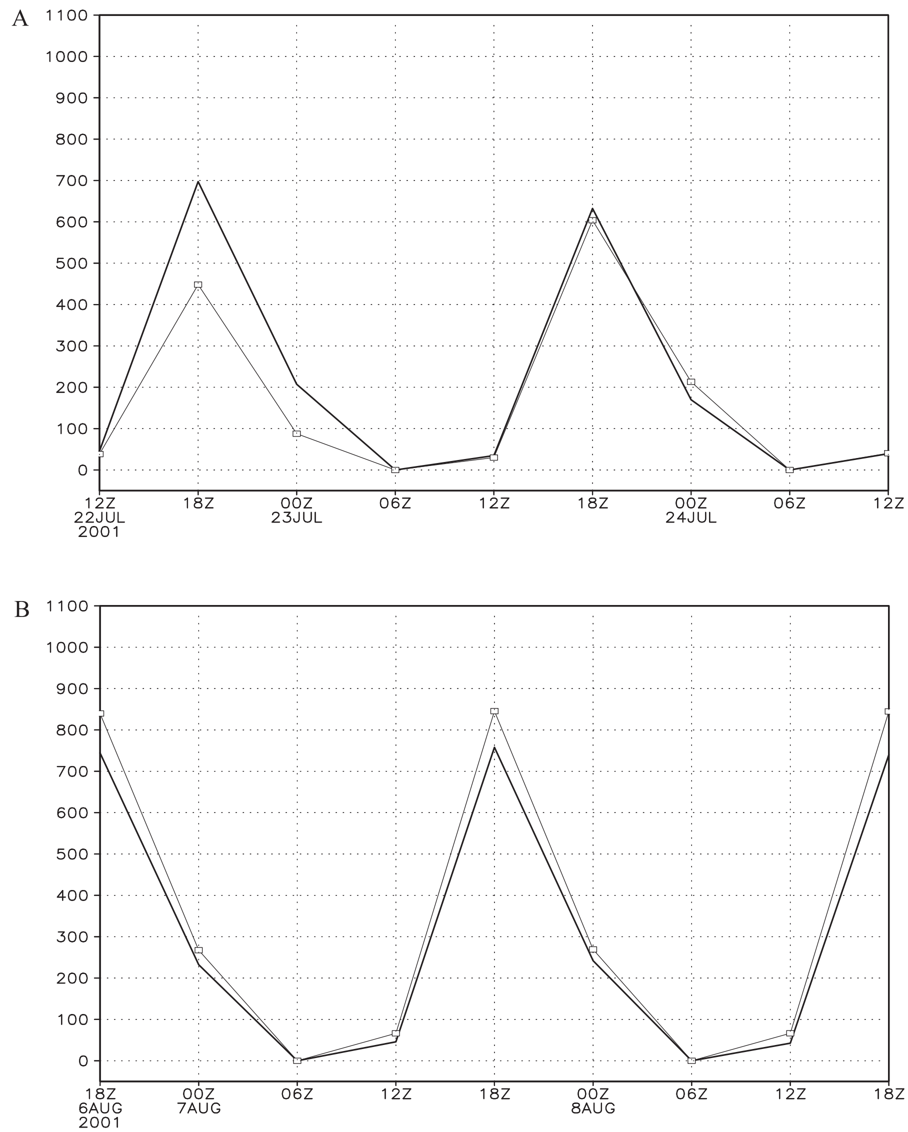

Fig. 10. Incoming shortwave radiation flux [W m^{-2}] derived from global model 24-h forecasts (thin line) for a cloudy period (A) and a clear-sky period (B). Observed values are indicated by thick lines.

rains. Figure 10 shows extracts from two periods, one in which observations and the global model indicated clear sky, and another in which the observations and global model forecasts indicated cloudy conditions. In the clear-sky period, the model overestimates the incoming shortwave radiation, whereas in cloudy periods these fluxes are underestimated.

The hourly observed values of incoming shortwave radiation peaked at approximately 900 W m^{-2}, and the hourly Eta forecasts of incoming shortwave radiation were similar to observed values. These forecasts showed a slow but steady increase toward the end of the dry season; this trend is not clear in the observations. A detailed assessment of cloudy and clear-sky periods predicted by the Eta Model shows that the excess of incoming solar radiation is larger on cloudy days (Fig. 11).

The mean diurnal cycle of shortwave incoming radiation predicted by the global model at 48 h is consistent with observed values (Fig.

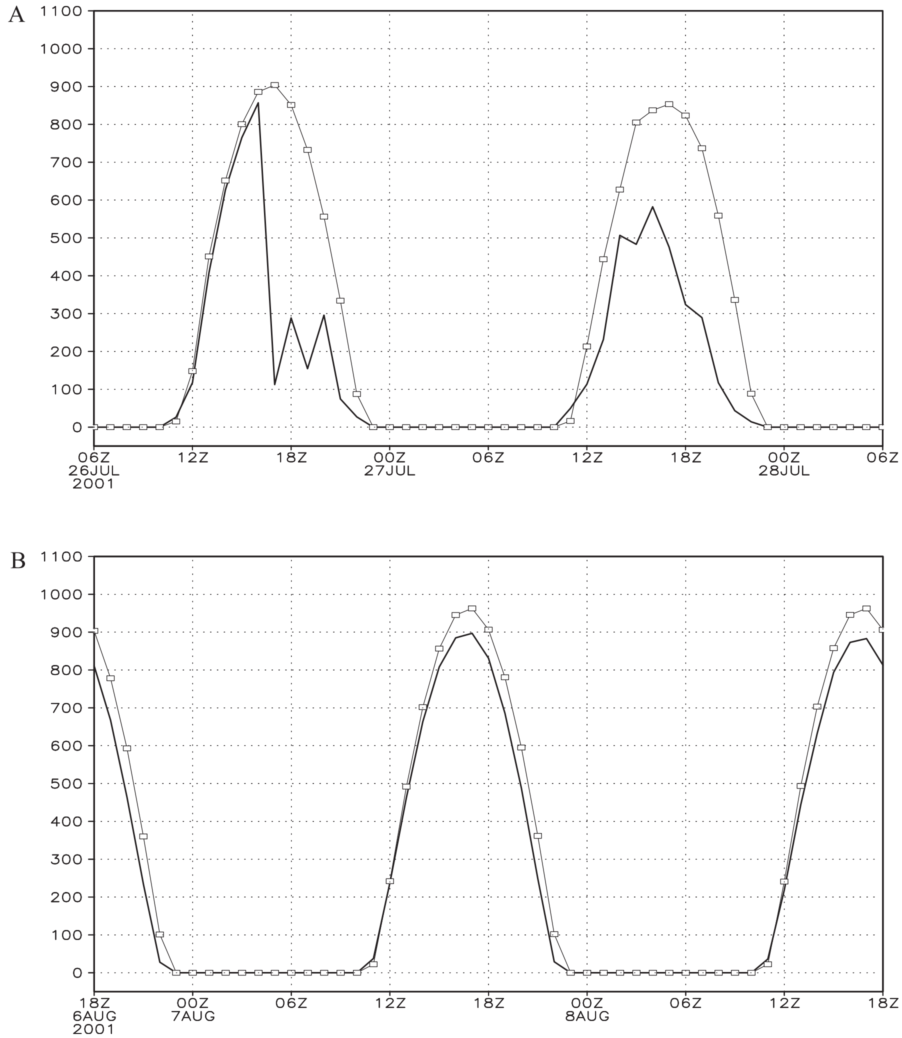

Fig. 11. Incoming shortwave radiation flux [W m^{-2}] derived from Eta Model 24-h forecasts (thin line) for a cloudy period (A) and a clear-sky period (B). Observed values are indicated by thick lines.

12); however, this occurred in the presence of frequent rains associated with deep convection. The mean diurnal cycle of incoming shortwave radiation predicted by the Eta Model (Fig. 12) showed that these fluxes were overestimated. A 1-h delay in these model fluxes is also apparent. This excess of incoming shortwave radiation has also been detected in different versions of the model (Hinkelman et al. 1999; Chou et al. 2002) when using the same radiation scheme.

The diurnal cycle of the global model 24-h forecasts of 6-hourly net radiation also showed a good fit with observations (Fig. 13). The global model correctly balances the radiation fluxes, as shown by the mean diurnal cycle of net radiation, but the partition between latent and sensible heat fluxes requires correction. In contrast, the Eta Model showed excessive net radiation in the diurnal cycle (Fig. 13). Overestimation of the Eta latent and sensible heat fluxes leads to an imbalance in the model heat budget. Figure 14 reveals that the imbalance is greater during the hours of sunrise and sunset, when flux residues reach approximately 30 W m^{-2} at around 12Z and 21Z.

In the Eta Model (Fig. 13), a clear 1-h delay in the forecast peaks occurred with the slow de-

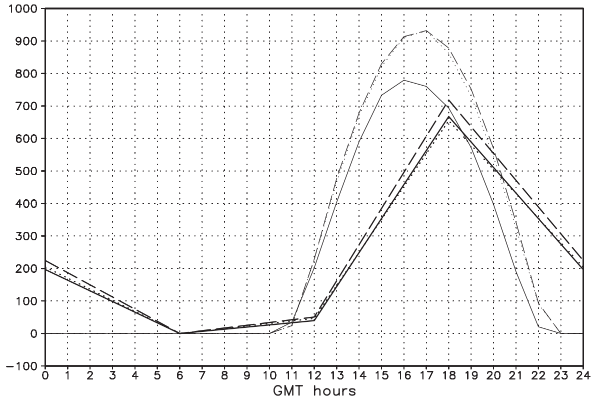

Fig. 12. Mean diurnal cycle of incoming shortwave flux [W m^{-2}] derived from 6-hourly mean observations (thick solid line), Global Model 24-h (thick dashed line) and 48-h (thick dotted line) forecasts, hourly observations (thin solid line), and Eta Model 24-h (thin dashed line) and 48-h (thin dotted line) forecasts.

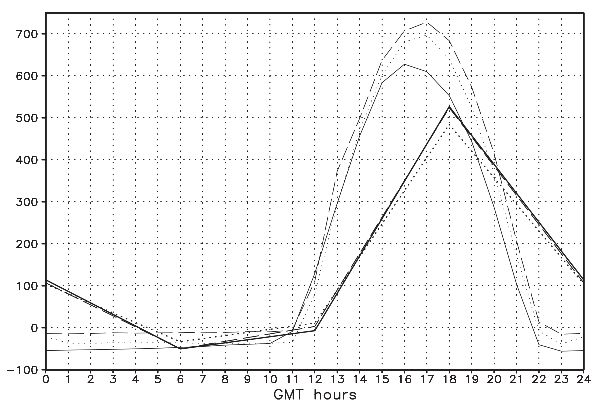

Fig. 13. Mean diurnal cycle of net radiation flux [W m^{-2}] derived from 6-hourly mean observations (thick solid line), global model 24-h (thick dashed line) and 48-h (thick dotted line) forecasts, hourly observations (thin solid line), and Eta Model 24-h (thin dashed line) and 48-h (thin dotted line) forecasts.

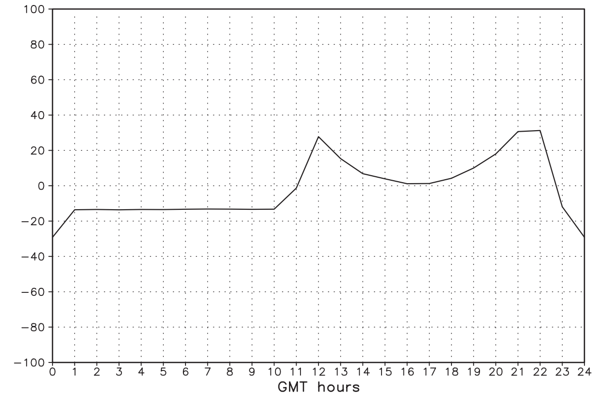

Fig. 14. Mean diurnal energy-budget residue [W m^{-2}] for 48-h forecasts of the Eta Model.

cay of the net radiation fluxes toward sunset, resulting in an overall overestimate. One would expect that afternoon clouds would reduce this excessive incoming solar radiation; however, this delay is present in the Eta forecast even during cloudless days. This indicates that the calculations of the solar zenith angle may require a revision. The nighttime net radiation is well forecast by both models, and no clear difference is observed in the quality of the 24-h and 48-h forecasts.

Table 4 shows that while the radiation fluxes of the global model are variable relative to observations, the Eta Model showed even greater variability. The mean errors of the global model were generally of smaller magnitude than those of the Eta Model, whereas the global model incoming shortwave and net radiation flux rmse were larger than those of the Eta Model. The 48-h global model forecasts showed an increase in negative bias related to increased cloud and precipitation production at this lead time.

4.5 Temperature

The global model near-surface temperature refers to the first model layer, as the model does not yet provide output at the 2-m level. The first layer of the global model is 60 m thick. Both models tended to overestimate the near-surface temperatures, particularly on those days when no precipitation was forecast by the models. The sharp reduction in temperature during the passage of frontal systems was captured by both models. Although the Eta Model predicted fewer rain events, the Eta 2-m temperature errors were larger than those for the global model. For a better comparison, a global model 2-m temperature should be derived; however, this can lead to increased error. The mean

Table 4. Standard deviation, bias error, root mean square error and correlation between observations and CPTEC GCM and Eta Model forecast time series of incoming shortwave radiation (SWinc) [W m^{-2}] and net radiation (netRad) [W m^{-2}].

Model	SD Obs	SD		BIAS		RMSE		CORR	
		24-h	48-h	24-h	48-h	24-h	48-h	24-h	48-h
CPTEC GCM SWinc	304.4	295.6	272.5	24.4	−1.8	171.4	164.5	0.84	0.84
CPTEC GCM netRad	261.6	232.6	211.2	−0.1	−7.4	132.9	131.6	0.86	0.87
Eta SWinc	267.5	357.7	353.2	55.5	50.6	114.0	111.6	0.97	0.97
Eta netRad	229.2	348.3	342.6	8.8	7.8	69.6	71.4	0.97	0.97

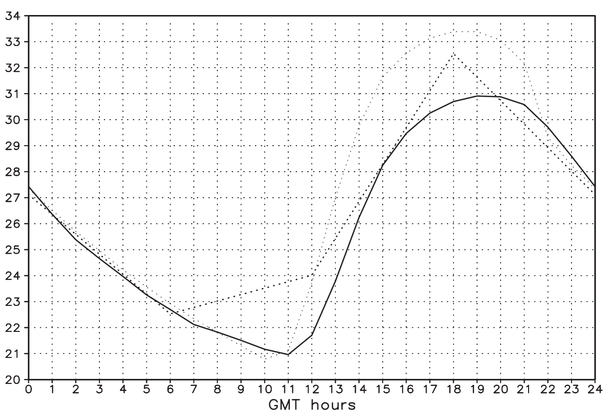

Fig. 15. Mean diurnal cycle of near-surface air temperature [°C] derived from hourly observations (thick solid line), Eta Model 48-h forecasts (thin dotted line), and 6-hourly 48-h forecasts from the global model (thick dotted line).

diurnal cycle shows that Eta forecasts exhibit a larger amplitude in the temperature cycle than observations (Fig. 15); a reduction in the incoming solar radiation could have helped to reduce this error. The 1-h delay in the Eta radiation peak is reflected in the surface temperatures, which on average also peak approximately 1 h after observed peaks. No clear improvement in the 48-h temperature forecasts are observed over the 24-h forecasts in either the Eta or global models.

Table 5 shows that the models and observations produced similar degrees of temperature variability. The errors in the Eta Model were larger than those in the global model but showed a stronger correlation with observations.

5. Discussion and conclusions

The CPTEC GCM and Eta Model were evaluated relative to surface observations undertaken at the CEOP Rondonia Reference Site located in the LBA area in Brazil for the period from 1 July to 1 September 2001, which is part of the Enhanced Observing Period 1 (EOP1).

Both models showed errors in precipitation forecasts; however, the global model greatly overestimated the monthly total amount and the number of events. The global model tended to show increased precipitation errors with forecast time, whereas the Eta Model produced underestimates that changed little with increasing forecast lead time. Although the coarse resolution of the global model is deficient in capturing convective clouds, the model produced frequent convective rain during the study period. The observed data revealed only three

Table 5. Standard deviation, bias error, root mean square error and correlation between observations and CPTEC GCM and Eta Model forecast time series of near-surface air temperature [°C].

Model	SD Obs	SD		BIAS		RMSE		CORR	
		24-h	48-h	24-h	48-h	24-h	48-h	24-h	48-h
CPTEC GCM	4.0	4.7	4.6	0.6	0.9	0.6	0.9	0.89	0.85
Eta Model	4.1	4.8	4.9	1.4	1.2	2.5	2.7	0.90	0.87

rain events, and the satellite-estimated cloud-top temperatures showed a lack of frequent organized deep convective clouds in the area surrounding the site, as suggested by the global model. In a model with such a coarse resolution as the global model, a convective cloud is assumed to occupy a small fraction of the grid cell. During summer, when convective clouds occur frequently, the probability that a grid cell contains a convective cloud is high; however, in dry periods when large areas are cloud-free, this probability is low. Therefore, the systematic presence of deep convection and precipitation in the global model, even at coarse resolution, can be considered a deficiency in dry periods.

The results showed that the latent heat fluxes of the global model are a direct response to precipitation that was made available as soil moisture. As the rain ceased, soil moisture declined to minimum values in less than 12 h. In reduced precipitation forecast periods, the global model failed to correctly reproduce the surface latent and sensible heat fluxes. A more highly efficient transfer of latent heat to the atmosphere should therefore be introduced into the global model. The latent heat fluxes of the global model are much smaller than the sensible heat fluxes; however, observations reveal that during dry periods the forest maintained its evapotranspiration rate and the latent heat fluxes were larger than the sensible heat fluxes. The net radiation was well predicted by the global model; however, the partition of this available surface energy between latent and sensible heat only approached observations when the global model produced rain at an excessive rate. An increase in the resolution of the global model could achieve considerable improvements in the forecasts, but a more realistic partition of latent and sensible heat fluxes in this Amazon forest area requires a reduction in the precipitation production and an increase in other sources of surface evaporation.

The root mean square error of the global model forecasts is generally equal to or smaller than the standard deviation of the observations, except for the latent and sensible heat fluxes. The rmse of the sensible heat flux of the global model is approximately three-times larger than its variability. The linear correlation between the observed and global forecast series is in excess of 0.6 for most of the variables, indicating a satisfactory correlation. The latent heat fluxes showed the smallest correlations. The forecast errors of the Eta Model show a positive bias for all variables. Although the biases of the Eta Model are generally greater than those of the global model, the Eta forecast rmse are mostly smaller than those of the global model. The Eta forecast rmse are also generally smaller than the variability in the observed data; therefore, the errors can be considered to be small. Correlation coefficients between observations and Eta forecasts for all variables are above 0.8. The correlations between Eta forecasts and observations are generally higher than those between the forecasts of the global model and observed values. We detected a number of differences in the quality of the 24-h forecasts of the global model relative to the 48-h forecasts; however, overall these two forecast lead times are of comparable quality, as they record similar values of rmse.

Although the integrations used the same initial conditions and the lateral boundary conditions were provided by the CPTEC GCM, the Eta limited-area model showed different error patterns from the global model; this shows that the errors were largely associated with model dynamics and the physics employed in the models. Although the Eta Model provided superior predictions of precipitation and did not show large errors in net radiation, the latent and sensible heat fluxes were significantly overestimated. This might indicate an imbalance in the Eta heat budget. This imbalance is in the order of 50 W m^{-2}, and occurs close to sunrise and sunset. The Eta Model also predicts dry-period latent heat fluxes that are larger than sensible heat fluxes, which is an expected feature in this region.

Systematic errors associated with the representation of orography in a coarse grid should be expected; however, errors in other model component such as radiation and land-surface scheme are more prominent than errors related to discrepancies in orography. The quality of the 48-h forecasts compared with the 24-h forecasts may have shown an improvement for certain variables, but overall we recognized no clear differences between the two forecasts; this indicates that only a minor increase in error is recorded in both models at short range.

The global model's radiation fluxes are more similar to observed values, but adjustments are required to the surface fluxes. The Eta Model requires correction of the excessive incoming shortwave radiation.

Acknowledgments

The authors would like to thank three reviewers for their comments and suggestions that helped to improve the manuscript.

References

Anthes, R.A. and D. Keyser, 1979: Tests of a finemesh model over Europe and the United States. *Mon. Wea. Rev*., **107**, 963–984.

Betts, A.K. and M.J. Miller, 1986: A new convective adjustment scheme. Part II: Single column tests using GATE wave, BOMEX and arctic air-mass data sets. *Quart. J. Roy. Meteor. Soc*., **112**, 693–709.

Betts, A.K., A.C.M. Beljaars, M.J. Miller, and P.A. Viterbo, 1996: The land-surface atmosphere interaction: A review based on observational and global modeling perspectives. *J. Geophys. Res*., **101**, 7209–7225.

Betts, A.K., F. Chen, E.K. Mitchell, and Z.I. Janjic, 1997: Assessment of the land surface and boundary layer models in two operational versions of the NCEP Eta Model using FIFE data. *Mon. Wea. Rev*., **125**, 2896–2916.

Bonatti, J.P., 1996: Modelo de Circulação Geral Atmosférico do CPTEC. *Climanálise*. Special Edition. INPE. São José dos Campos.

Bosilovich, M.G. and R. Lawford, 2002: The Coordinated Enhanced Observing Period (CEOP) International Workshop. *Bull. Amer. Meteor. Soc*., **83**, 1495–1499.

Bustamante, J.F.F., J.L. Gomes, S.C. Chou, and J.R. Rozante, 1999: Evaluation of April 1999 rainfall forecasts over South America using the Eta Model. *Climanálise*, 1999.

Cavalcanti, I.F.A., J.A. Marengo, P. Satyamurty, I. Trosnikov, J.P. Bonatti, C.A. Nobre, C. D'Almeida, G. Sampaio, C.A.C. Cunningham, H. Camargo, and M.B. Sanches, 2002: Climatological features represented by the CPTEC/COLA Global Climate Model. *J. Climate*, **15**, 2965–2988.

Chen, F., Z.I. Janjic, and K. Mitchell, 1997: Impact of atmospheric surface-layer parameterization in the new land-surface scheme of the NCEP mesoscale Eta Model. *Bound. Layer Meteor*., **85**, 391–421.

Chou, S.C., C.A.S. Tanajura, Y. Xue, and C.A. Nobre, 2002: Validation of the Eta/SSiB over South America. *J. Geophys. Res*., **107**, D20.

Fels, S.B. and M.D. Schwarzkopf, 1975: The simplified exchange approximation. A new method for radiative transfer calculations. *J. Atmos. Sci*., **32**, 1475–1488.

Gates, W.L., J. Boyle, C. Covey, C. Dease, C. Doutriaux, R. Drach, M. Fiorino, P. Gleckler, J. Hnilo, S. Marlais, T. Phillips, G. Potter, B. Santer, K. Sperber, K. Taylor and D. Williams, 1998: An Overview of the Results of the Atmospheric Model Intercomparison Project (AMIP I), *Bull. Amer. Meteor. Soc.*, **73**, 1962–1970.

Harshvardhan, Davies, R., D.A. Randall, and T.G. Corsett, 1987: A fast radiation parameterization for atmospheric circulation models. *J. Geophys. Res*., **92**, 1009–1016.

Hinkelman, L.M., T.P. Ackerman, and R.T. Marchand, 1999: An evaluation of the NCEP Eta Model predictions of surface energy budget and cloud properties by comparison with measured ARM data. *J. Geophys. Res*., **104**, D16, 19535–19549.

Janjic, Z.I., 1994: The step-mountain eta coordinate model: further developments of the convection, viscous sublayer and turbulence closure schemes. *Mon. Wea. Rev*., **122**, 927–945.

Lacis, A.A. and J.E. Hansen, 1974: A parameterization for the absorption of solar radiation in the Earth's atmosphere. *J. Atmos. Sci*., **31**, 118–133.

Marengo, J.A. and L. Horta, 2003: CEOP reference sites in LBA Continental Scale Experiment. *CEOP Newsletter*, **4**, 6.

Machado, L.A., W.B. Rossow, R.L. Guedes, and A.W. Walker, 1998: Life cycle variations of mesoscale convective systems over the Americas. *Mon. Wea. Rev.*, **126**, 1630–1654.

Marengo, J., I.F.A. Cavalcanti, P. Satyamurty, C.A. Nobre, J.P. Bonatti, A. Manzi, I. Trosnikov, G. Sampaio, H. Camargo, M.B. Sanches, C.A.C. Cunningham, C. D'Almeida, and L.P. Pezzi, 2003: Ensemble simulation of regional rainfall features in the CPTEC/COLA atmospheric GCM. Skill and Predictability assessment and applications to climate predictions. *Climate Dynamics*, **21**, 459–475.

Mesinger, F., 1984: A blocking technique for representation of mountains in atmospheric models. *Riv. Meteor. Aeronaut*., **44**, 195–202.

Mesinger, F., Z.I. Janjic, S. Nickovic, D. Gavrilov, and D.G. Deaven, 1988: The step-mountain coordinate: Model description and performance for cases of Alpine lee cyclogenesis and for a case of Appalachian redevelopment. *Mon. Wea. Rev*., **116**, 1493–1518.

Negri, A.J., R.F. Adler, and L. Xu, 2002: A TRMM-calibrated infrared rainfall algorithm applied over Brazil. *J. Geophys. Res*., **107**, D20.

Rebello, E.R.G., N.D. Sales, M.G.R. Oliveira, and M.S.B. Ribeiro, 1996: Mean charts of rainy days in Brazil (Mapas médios dos números de dias chuvosos do Brasil). Instituto Nacional de Meteorologia, 70610-400, Brasília, DF. Brazil.

Sestini, M.F., R.C.S. Alvalá, E.M.K. Mello, D.M. Valeriano, S.C. Chou, C.A. Nobre, J.A.C. Paiva, and É.S. Reimer, 2002. Vegetation map elaboration for use in numerical models ("Elaboração de mapas de vegetação para utilização em modelos meteorológicos e hidrológicos"). Internal Report. Instituto Nacional de Pesquisas Espaciais, São José dos Campos, SP. Brazil.

Shuttleworth, W.J., J.H.C. Gash, C.R. Lloyd, A.O. Marques Filho, G. Fisch, V.P. Silva Filho, M.N.G. Ribeiro, L.C. Molion, L.D.A. Sá, C.A. Nobre, O.M. Cabral, S. Patel, and J.C. de Moraes, 1984: Eddy correlation measurements of energy partition for Amazonian forest. *Quart. J. R. Met. Soc*., **110**, 1143–1162.

Takle, E.S., W.J. Gutowski, Jr., R.W. Arritt, Z. Pan, C.J. Anderson, R. Silva, D. Caya, S.-C. Chen, J.H. Christensen, S.-Y. Hong, H.-M.H. Juang, J.J. Katzfey, W.M. Lapenta, R. Laprise, P. Lopez, J. McGregor, and J.O. Roads, 1999: Project to Intercompare Regional Climate Simulations (PIRCS): Description and initial results. *J. Geophys. Res.*, **104**, **19**, 443–19, 462.

Xue, Y., J.P. Sellers, J.L. Kinter III, and J. Shukla, 1991: A simplified simple biosphere model for global climate studies, *J. Climate*, **4**, 345–364.

Xue, Y., H.G. Bastable, P.A. Dirmeyer, and P.J. Sellers, 1996: A sensitivity study of simulated surface fluxes to changes in land surface parameterization—A study using ABRACOS data. *J. Appl. Meteor*., **35**, 386–400.